Geochemistry, Geophysics, Geosystems

RESEARCH ARTICLE
10.1029/2020GC009132

Ventilation History of the Nordic Seas Deduced From Pelagic-Benthic Radiocarbon Age Offsets

Maciej M. Telesiński[1], Mohamed M. Ezat[2,3,4], Francesco Muschitiello[5,6], Henning A. Bauch[7], and Robert F. Spielhagen[8]

[1]Institute of Oceanology Polish Academy of Sciences, Sopot, Poland, [2]CAGE – Centre for Arctic Gas Hydrate, Environment and Climate, Department of Geosciences, UiT, The Arctic University of Norway, Tromsø, Norway, [3]Godwin Laboratory for Palaeoclimate Research, Department of Earth Sciences, University of Cambridge, Cambridge, UK, [4]Department of Geology, Faculty of Science, Beni-Suef University, Beni-Suef, Egypt, [5]Department of Geography, University of Cambridge, Cambridge, UK, [6]NORCE Norwegian Research Centre, Bergen, Norway, [7]Alfred Wegener Institute for Polar and Marine Research, c/o GEOMAR Helmholtz Centre for Ocean Research, Kiel, Germany, [8]GEOMAR Helmholtz Centre for Ocean Research, Kiel, Germany

Key Points:

- We present four radiocarbon ventilation age records of subsurface and bottom waters from the Nordic Seas since the Last Glacial Maximum
- Planktic records are generally older than modern but show significant spatial variability, indicating the influence of local conditions in some intervals
- Benthic records show weaker ventilation during stadials and stronger during interstadials, reflecting shifts in overturning circulation

Supporting Information:

Supporting Information may be found in the online version of this article.

Correspondence to:

M. M. Telesiński,
mtelesinski@iopan.pl

Citation:

Telesiński, M. M., Ezat, M. M., Muschitiello, F., Bauch, H. A., & Spielhagen, R. F. (2021). Ventilation history of the Nordic Seas deduced from pelagic-benthic radiocarbon age offsets. *Geochemistry, Geophysics, Geosystems*, *22*, e2020GC009132. https://doi.org/10.1029/2020GC009132

Received 26 MAY 2020
Accepted 9 DEC 2020

Abstract Changes in ocean circulation are considered a major driver of centennial-to-millennial scale climate variability during the last deglaciation. Using four sediment records from the Nordic Seas, we studied radiocarbon ventilation ages in subsurface and bottom waters to reconstruct past variations in watermass overturning. Planktic foraminiferal ages show significant spatial variability over most of the studied period. These differences suggest that the ventilation of the shallower subsurface waters is strongly influenced by local conditions such as sea-ice and meltwater input, changes in mixed-layer depth, and/or variable contributions of water masses with different ^{14}C signatures. Despite covering a significant water depth range, the benthic foraminiferal records show common long-term patterns, with generally weaker ventilation during stadials and stronger during interstadials. The Greenland Sea record differs the most from the other records, which can be explained by the greater depth and the geographical distance of this site. The benthic records reflect regional shifts in deep convection and suggest that the deep Nordic Seas have been generally bathed by a single, though changing, deep-water mass analogous to the present-day Greenland Sea Deep Water. Since significant offsets in ventilation ages are yielded by different taxonomic or ecological groups of benthic foraminifera, the use of uniform material seems a prerequisite to reconstruct bottom water ventilation histories.

Plain Language Summary Earth's climate is tightly coupled with the global ocean conveyor belt. To understand climate changes, we need to reconstruct past ocean circulation. A suitable place to perform such studies is the Nordic Seas. We analyze four sediment records of the last deglaciation (~20–10 thousand years ago) during which the Earth's climate experienced a transition from an ice age to a warm period, with several plot twists in between. We compare radiocarbon ages of shells of organisms that have lived on the bottom of the sea and close to its surface. As these fossils are found in the same sediment layers, they lived at the same time in the geological past. However, their radiocarbon ages differ. The amount of this difference depends on the intensity of water exchange between the surface and the bottom of the ocean. From the difference we infer the pace of deep-water formation. Our results show intensive ocean circulation during the relatively warm periods and a weaker exchange of water masses during relatively cold periods. The outcomes of our study might help to improve computer models of the ocean-climate system and allow us to predict with greater confidence its changes in the future.

1. Introduction

Between ~20 and 10 thousand years, before 1950 CE (ka), Earth's climate underwent a shift from a glacial maximum to interglacial conditions (e.g., Clark et al., 2012; CLIMAP Project Members, 1976). This transition, interrupted by climatic anomalies such as Heinrich Stadial 1 (HS1) and the Younger Dryas (YD) stadial (Dansgaard et al., 1993; Shakun et al., 2012), was strongly coupled with regional changes in ocean circulation (e.g., McManus et al., 2004; Skinner et al., 2014, 2019). An important component of the ocean-climate system is the Atlantic Meridional Overturning Circulation (AMOC). Its variability is thought to have played

an important role in these millennial-scale climate anomalies as it affects the global heat transport and air–sea gas exchange (e.g., Broecker, 1998).

Within the North Atlantic region, the Nordic Seas is an area particularly important for the AMOC and, thus, well suited for the study of its variability. First, the Nordic Seas constitutes the main surface and the only deepwater connection between the Arctic and the Atlantic oceans (Håvik et al., 2017; Swift, 1986). Warm and saline Atlantic Water (AW) is advected northward by the North Atlantic Current, transporting large amounts of heat in the eastern Nordic Seas, while cold and less saline water flowing southward as the East Greenland Current carries sea ice and icebergs into their western part. Second, the Nordic Seas is one of the few areas worldwide where open-ocean convection and deepwater formation occur (Marshall & Schott, 1999; Rudels & Quadfasel, 1991). The northward flowing AW loses heat, becomes dense enough to sink to the bottom, and contributes significantly to the renewal of lower North Atlantic Deep Water—one of the most important water masses of the AMOC (Aagaard et al., 1985; Hansen & Østerhus, 2000; R. R. Dickson & Brown, 1994). The sea ice advected from the Arctic plays an important role in preconditioning the deep convection (Marshall & Schott, 1999).

Changes in ocean circulation and air-sea gas exchange can be reconstructed using radiocarbon ventilation ages, which reflect the radiocarbon age difference between ocean water and the atmosphere. The ocean-atmosphere ^{14}C disequilibrium is a direct expression of changes in the rate of air-sea gas equilibration, deep-water renewal and mixing, and changes in water sources (e.g., Adkins & Boyle, 1997; Skinner et al., 2019). The intensity of deep convection and, thus, the thermohaline circulation in the North Atlantic changes over different timescales from interannual (R. Dickson et al., 1996) to millennial (e.g., Skinner & Shackleton, 2004; Stern & Lisiecki, 2013; Telesiński et al., 2015). During the last glacial, the overturning circulation in the Nordic Seas was weak but active (e.g., Ezat et al., 2019), and it collapsed completely during HS1 (McManus et al., 2004). The onset of the Bølling-Allerød (BA) interstadial was marked by a resumption of the deep water formation (Ezat et al., 2017), which declined into the YD stadial (McManus et al., 2004).

Here, we present a comparison of four radiocarbon ventilation age records from the central and southern Nordic Seas (Figure 1), covering the last deglaciation (21.9 ka). Three previously published records include cores PS1243 (Thornalley et al., 2015), JM11-FI-19PC (Ezat et al., 2017), and MD99-2284 (Muschitiello et al., 2019). The PS1878 ventilation age record is presented here for the first time. The advantage of this site is that it is located close to the present-day convection center (Marshall & Schott, 1999; Telesiński, Spielhagen, & Lind, 2014), allowing a direct reconstruction of deep convection changes.

2. Material and Methods

2.1. Chronology

As the base for the chronological framework of the presented records, we use core MD99-2284 as this record exhibits the highest temporal resolution and has a robust chronology established by aligning variations in downcore sea-surface temperatures with synchronous changes in the hydroclimate record from southern Sweden (Muschitiello et al., 2020) in the interval between 10 and 14.8 ka. For the older part of the records, we use the chronology of core JM11-FI-19PC, which was previously aligned with the North Greenland Ice Core Project (NGRIP) ice core based on tephras, $\delta^{18}O$, magnetic susceptibility, and K/Ti records (Ezat et al., 2014, 2017). To align the chronologies of the presented cores, we use their published planktic $\delta^{18}O$ records based on *Neogloboquadrina pachyderma* (Bakke et al., 2009; Bauch et al., 2001; Ezat et al., 2016; Hoff et al., 2016; Telesiński, Spielhagen, & Lind, 2014). We correlate the records using visual tie points as well as the Saksunarvatn ash, which is present in cores JM11-FI-19PC and MD99-2284, and the Vedde ash, which is found in JM11-FI-19PC, MD99-2284, and PS1243 (Figure 2).

The bottom-most part of core PS1878 was correlated with the onset of the interval of high and stable $\delta^{18}O$ values in cores PS1243 and JM11-FI-19PC at 20.8 ka (Figure 2). Although this is an uncertain tie, the lack of a characteristic structure in this part of the record does not allow for a more accurate correlation. The resulting sedimentation rates are relatively high (c. 10.5 cm/kyr, Figure S1) but reasonable, especially taking into account high IRD abundance in this interval (Telesiński, Spielhagen, & Lind, 2014). The rapid $\delta^{18}O$ decrease, most probably associated with the onset of HS1, was correlated with similar features in other records dated to 18.5–17.1 ka. The extremely low $\delta^{18}O$ values between c. 16 and 14 ka in core PS1878 are

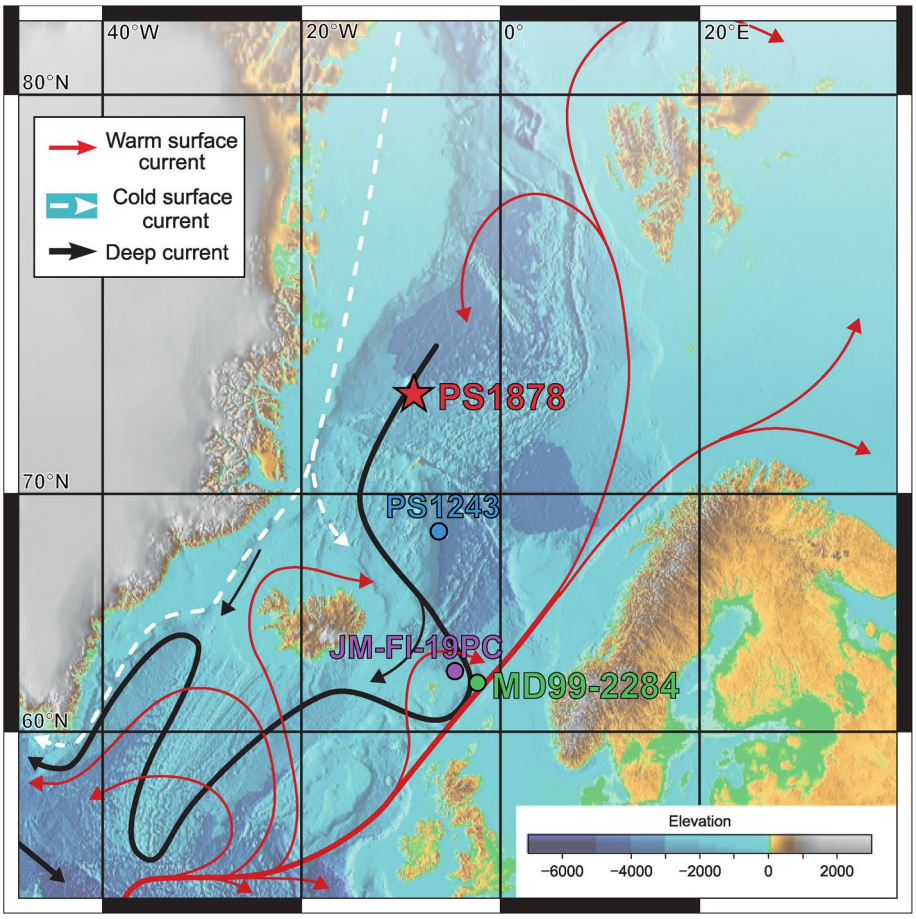

Figure 1. Map of major surface and bottom water currents in the northern North Atlantic and the Nordic Seas (Hansen & Østerhus, 2000). Location of studied cores PS1878 (3,048 m water depth; red star; Telesiński, Spielhagen, & Lind, 2014), PS1243 (2,711 m water depth; blue circle; Bauch, Erlenkeuser, et al., 2001), JM11-FI-19PC (1,179 m water depth; purple circle; Ezat et al., 2014) and MD99-2284 (1,500 m water depth; green circle; Muschitiello, D'Andrea, Schmittner, et al., 2019).

interpreted as a local feature that cannot be correlated to other distant records (Telesiński et al., 2015). The subsequent tie points include the transition from low to high $\delta^{18}O$ values after the end of HS1 (13.8 ka), a small but prominent light $\delta^{18}O$ peak at 13.5 ka and the light $\delta^{18}O$ peak related to the YD stadial at 12.1 ka. In cores JM11-FI-19PC, MD99-2284, and PS1243 the latter is also marked by the presence of the Vedde ash (Figure 2). The correlation between cores JM11-FI-19PC and MD99-2284 includes more tie points due to the higher temporal resolution of these two records (Figure 2). The original, radiocarbon-based age models with a reservoir age of 400 years were used for the mid-to late Holocene (<9 ka) part of the PS1878 (Telesiński et al., 2015), PS1243 (Bauch et al., 2001), and JM11-FI-19PC (Ezat et al., 2014) records as the structure of the $\delta^{18}O$ records does not allow for a well-defined correlation. However, it is generally agreed that at least since c. 9 ka ocean circulation and, thus, the planktic reservoir ages were similar to today (e.g., Thornalley et al., 2015; Waelbroeck et al., 2001). Nevertheless, our ventilation age reconstruction is limited to the interval from the Last Glacial Maximum (LGM) to the early Holocene, that is, 21.9 ka. A comparison of sedimentation rates between the original age models and the ones used in this study is shown for each core in Figure S1.

AMS ^{14}C dates of *N. pachyderma* in the interval 42.5–45.5 cm (c. 9.5–10.9 ka) of core PS1878 yielded reversed ages (Table S1). Because the sediment material in this core section may have been affected by bioturbational activities e.g., vertical burrowing, this interval is omitted in the discussion.

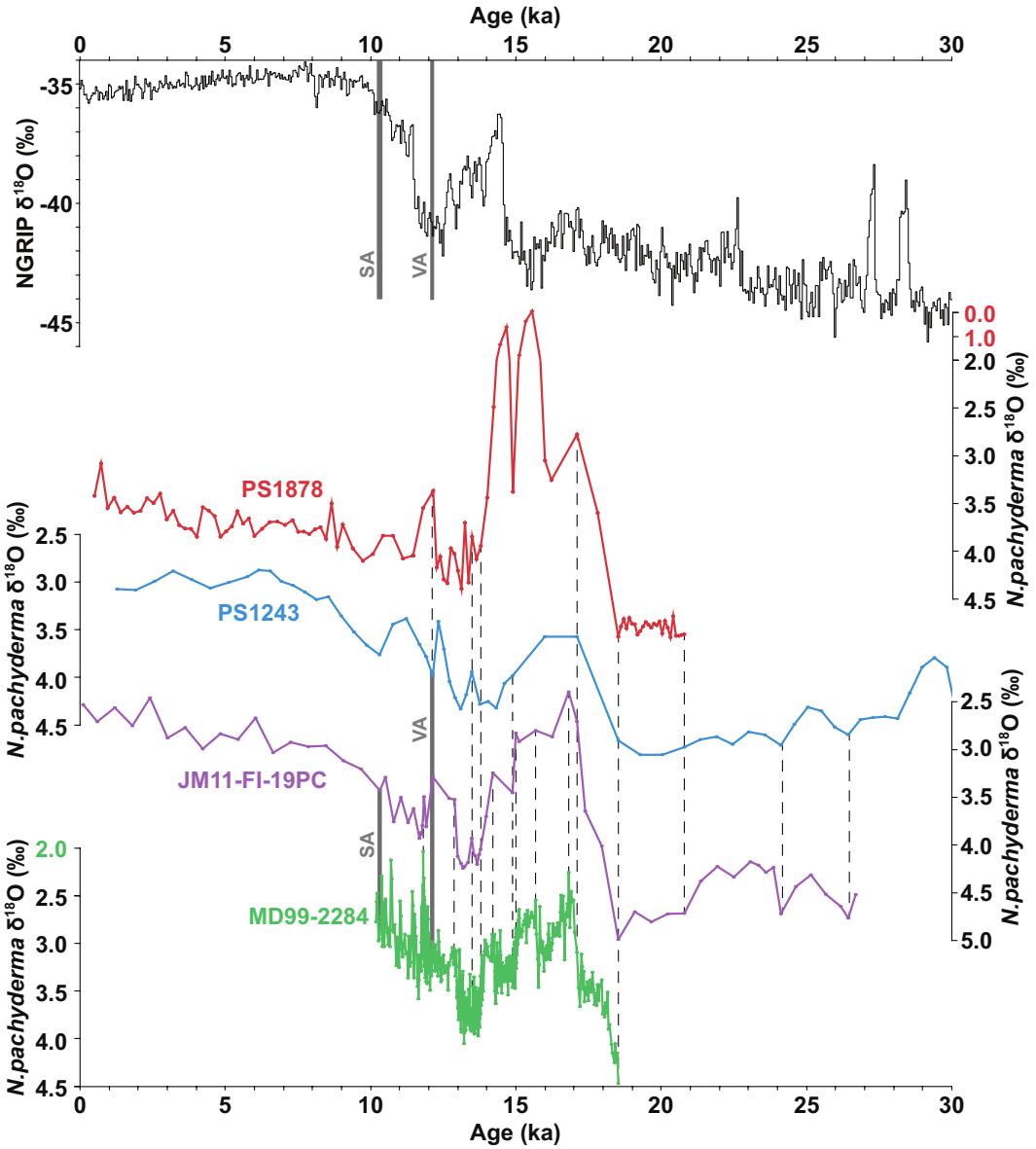

Figure 2. (a) The NGRIP ice cores $\delta^{18}O$ record (Andersen et al., 2004) plotted along with planktic $\delta^{18}O$ records of cores (b) PS1878, (c) PS1243, (d) JM11-FI-19PC, and (e) MD99-2284. Dashed lines indicate tie points used for the visual correlation of the records. Gray vertical bars indicate ash layers used for the correlation. SA, Saksunarvatn Ahs; VA, Vedde Ash.

2.2. Ventilation Age Reconstructions

Core PS1878 from the central Greenland Sea (Figure 1) has been shown to contain a continuous record of submillennial resolution, covering the interval from the LGM until present (Telesiński, Spielhagen, & Lind, 2014; Telesiński, Spielhagen, & Bauch, 2014; Telesiński et al., 2015). For the present study, four previously published AMS ^{14}C dates on planktic foraminifera *N. pachyderma* (Telesiński, Spielhagen, & Lind, 2014; Telesiński et al., 2015) were used for reservoir age calculations. Seven additional planktic samples and 18 benthic samples (two samples consisting of epifaunal species *Cibicidoides wuellerstorfi*, five samples of shallow infaunal species *Oridorsalis umbonatus*, and seven samples of miliolid *Pyrgo* spp.) were dated at the Poznan Radiocarbon Laboratory, the National Ocean Sciences Accelerator Mass Spectrometry (NOSAMS) facility and the Alfred Wegener Institute (Table S1). All samples contained only pristine specimens of the selected taxa (or, in a few cases, also minor amounts of other taxa, see Table S1).

The reconstructions were generated by propagating chronological and analytical errors were propagated using a statistical approach. Radiocarbon ventilation ages were estimated using a random walk model fitted via Markov chain Monte Carlo (MCMC) and taking into account both calendar age uncertainty and ^{14}C measurements errors. Our random walk model (RWM) has been successfully employed to estimate and compare ^{14}C ventilation histories from deep-sea sediments and corals from the last deglaciation, and a full mathematical formalism can be found in Muschitiello et al. (2019). We reconstruct shallow subsurface (~100 m water depth or more, especially at times of thicker halocline, cf. Greco et al., 2019) reservoir ages using *N. pachyderma* and bottom water ^{14}C ventilation ages using infaunal and epifaunal nonmiliolid benthic foraminifera. Hereafter, we will refer to these ages as Planktic-Atmosphere (P-Atm) and Benthic-Atmosphere (B-Atm) ventilation ages, respectively. We also determine the difference between paired benthic and planktic ^{14}C dates to determine the age difference between the subsurface and the bottom water, hereafter referred to as the Benthic-Planktic (B-P) age offset.

We also recalculated the previously published ventilation ages of cores JM11-FI-19PC, MD99-2284, and PS1243 (Ezat et al., 2017; Muschitiello et al., 2019; Thornalley et al., 2015, respectively) according to the modified age models, using the same RWM (Table S2). In the case of core PS1243, we calculated only P-Atm reservoir ages as the benthic samples of this record consisted of both miliolid and nonmiliolid foraminifera (Thornalley et al., 2015, see the discussion in, Ezat et al., 2017).

Each stratigraphic tie-point used for the marine–marine ($\delta^{18}O_{Np}$–$\delta^{18}O_{Np}$) and marine–ice core ($\delta^{18}O_{Np}$–$\delta^{18}O_{ice}$) correlations is generally associated with a non-negligible error on the depth scale. This is because the sampling resolution across records does not match. Here, we adopt a similar methodology as that devised by Olsen et al. (2014) and assume that the error in depth can be constrained by neighboring sampling data points, that is, the maximum depth difference between a given tie point measurement and the two adjacent sampling levels that straddle the tie point. We assign an error corresponding to 1σ, which is twofold more conservative than that used by Olsen et al. (2014), who assigned a 2σ error. After synchronization to the dated records using the tie points discussed above, we converted the depth error in the age domain and estimated the uncertainty associated with our tie-points as follows: 160 years for PS1878, 450 years for PS1243, 190 years for JM11-F1-19PC, and 25 years for MD99-2284 (note that this core has an average sampling resolution of ~5–10 years per measurement). These uncertainty estimates were ultimately incorporated into the RWM used to estimate the ventilation ages described above.

3. Results and Discussion

While the B-Atm ventilation ages of epifaunal *C. wuellerstorfi* (B_{Cw}-Atm) and infaunal *O. umbonatus* (B_{Ou}-Atm) in core PS1878 were <2700 ^{14}C years throughout the record, the miliolid *Pyrgo* species (mostly *Pyrgo depressa*) yielded ventilation ages of up to c. 12,000 ^{14}C years (Table S1). It has been observed before that *Pyrgo* and most probably other miliolid species yield radiocarbon ages much older than the co-occurring nonmiliolid species (e.g., Ezat et al., 2017; Heier-Nielsen et al., 1995; Vorren & Plassen, 2002). The issue has been comprehensively discussed by Ezat et al. (2019), and here, we refrain from using the *Pyrgo* ventilation ages for the reconstruction of past bottom water ventilation.

In cores PS1878 and JM11-FI-19PC, dating of different nonmiliolid benthic foraminiferal species or ecological groups from the same sample yielded varying ventilation ages (Figures 4a and 4b and Tables S1 and S2). In PS1878, the epifaunal foraminifera yielded lower ventilation ages. In the JM11-FI-19PC record, the epifaunal dates are c. 200–400 ^{14}C years older than the infaunal species, which could largely be explained by the differences in species habitat, given the sedimentation rates. All the observed differences exceed estimated errors. Except for one case in core PS1878 described below, we use all B-Atm ages from nonmiliolid foraminifera for the ventilation history reconstruction. However, we recommend using, if possible, narrow and uniform taxonomic or ecological groups of foraminifera for the reconstruction of bottom water ventilation.

During the LGM and the onset of the deglaciation (21–18 ka), the P-Atm values of PS1878 were relatively low, oscillating around c. 500 ^{14}C years (Figure 3a and Table S1). These values are in good agreement both with JM11-FI-19PC and PS1243 (Figures 3b and 3c) though it should be kept in mind that the tie point used to correlate the bottom-most part of the PS1878 record is fairly uncertain (see above) and so are the

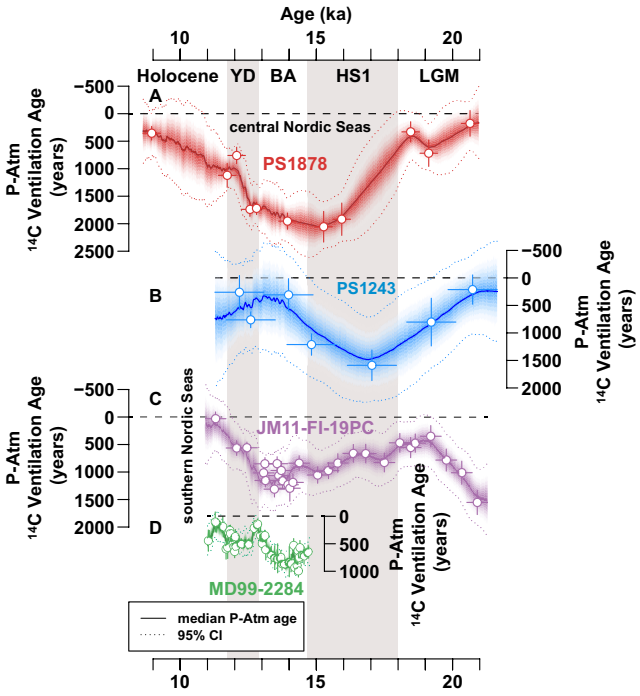

Figure 3. Planktic-Atmosphere (P-Atm) reservoir age estimates of cores (a) PS878, (b) PS1243, (c) JM11-FI-19PC, and (d) MD99-2284. Shading reflects the 95% posterior credible interval (2σ) of ^{14}C ventilation as a function of age found by MCMC using random walk model (see Section 2.2 for details) and taking into account analytical and chronological uncertainty in our observed data. Stratigraphic units are indicated at the top. BA, Bølling-Allerød interstadial; HS1, Heinrich Stadial 1; LGM, Last Glacial Maximum; YD, Younger Dryas stadial.

resulting reservoir ages. Nevertheless, the ventilation of the uppermost water column both in the southern and in the central Nordic Seas was in a range similar to modern values of ~400 years. The B-Atm ages in JM11-FI-19PC (≥1,000 ^{14}C years, Figure 4b) were significantly higher than at present (~500 years, e.g., Hansen & Østerhus, 2000; Mangerud et al., 2006). Altogether, the data seem to confirm the active, though weak Nordic Seas overflows suggested for this period (Ezat et al., 2017). However, it remains unclear whether the well-ventilated surface water originated from vertical convection or was laterally advected from the south (e.g., Rasmussen et al., 1996). The latter is evidenced by the occurrence of the small-sized subpolar species *Turborotalita quinqueloba* in core PS1243 (Bauch et al., 2012; Thibodeau et al., 2017).

During HS1, the P-Atm reservoir ages increased significantly both in the southern and in the central Nordic Seas (Figure 3). In the PS1243 record, the P-Atm values rose to c. 1,500 ^{14}C years already around 17.1 ka. This trend is in agreement with the PS1878 record where the values increased to >1,900 ^{14}C years after 16 ka. Extremely low planktic $\delta^{18}O$ values between 18 and 14 ka in core PS1878 (Figure 2b) suggest the presence of a freshwater and sea-ice lid in the central Nordic Seas throughout this period (Telesiński et al., 2015), which could have hampered air-sea gas exchange and ventilation of subsurface waters. In core JM11-FI-19PC, the P-Atm reservoir ages increased gradually to reach c. 1,000 ^{14}C years at the end of HS1 (Figure 3c), indicating a less pronounced ventilation weakening. The B-Atm ventilation ages in the southern Nordic Seas (core JM11-FI-19PC) also increased over HS1 to reach a maximum of c. 2,000 ^{14}C years at 15.4 ka (Figure 4b). This value is in agreement with that from core MD99-2284 (c. 2,100 ^{14}C years at 14.7 ka, Figure 4c). Unfortunately, the lack of reliable benthic ventilation age estimates in the PS1878 record precludes conclusions on the ventilation changes over HS1. Nevertheless, extremely high P-Atm ventilation ages over HS1 in core PS1878 and B-Atm ventilation ages in late HS1/early BA in all three records suggest a significant reduction of deepwater formation in the Greenland Sea during this stadial. Most probably, large amounts of freshwater and sea ice that affected the areas of deepwater formation for ~4,000 years (Figure 2) created a halocline strong enough to prevent deep convection (Sarnthein et al., 1995; Telesiński, Spielhagen, & Lind, 2014; Telesiński et al., 2015). As a result, the meridional circulation in the Nordic Seas slowed down (McManus et al., 2004; Stanford et al., 2011), resulting in limited AW inflow, reduced Nordic Seas overflow, and a gradually decreasing ventilation of bottom and subsurface waters also in the southern Nordic Seas.

In the PS1243 record, the P-Atm reservoir ages decreased below 500 ^{14}C years after the end of HS1 (Figure 3b). A shift of similar timing and amplitude was observed in a record from the eastern Nordic Seas and associated with the collapse of marine-based sectors of the Eurasian Ice Sheet (Brendryen et al., 2020). In contrast, in the southern Nordic Seas, the P-Atm ventilation ages continued to increase and reached maximum values of 500–1,000 ^{14}C years in MD99-2284 and 1,000–1,500 ^{14}C years in JM11-FI-19PC only around 13.5–14 ka, that is, in the middle of the BA interstadial (Figures 3c and 3d). An offset largely exceeding the estimated uncertainties can be observed between the two southernmost records around this time (median values of c. 700 vs. 1,100 ^{14}C years, respectively). Although quite small compared to the temporal variability of both records, the difference is noteworthy taking into account the small distance between the two sites (only c. 150 km apart). We hypothesize that more sea ice and meltwater accumulated on the lee side of the Faroe Islands (relative to the dominant ocean current direction, see Figure 1), where site JM11-FI-19PC is located, leading to increased ventilation ages. Site MD99-2284, located in the main flow of the NAC, remained ice-free over the discussed time interval, resulting in much better ventilation. At present, however, more robust conclusions cannot be drawn from the available data. The divergence of the central Greenland Sea record is less surprising, taking into account the geographical distance and the different oceanographic regime of this site with a strong influence of freshwater. Despite a slight decrease compared to HS1, the

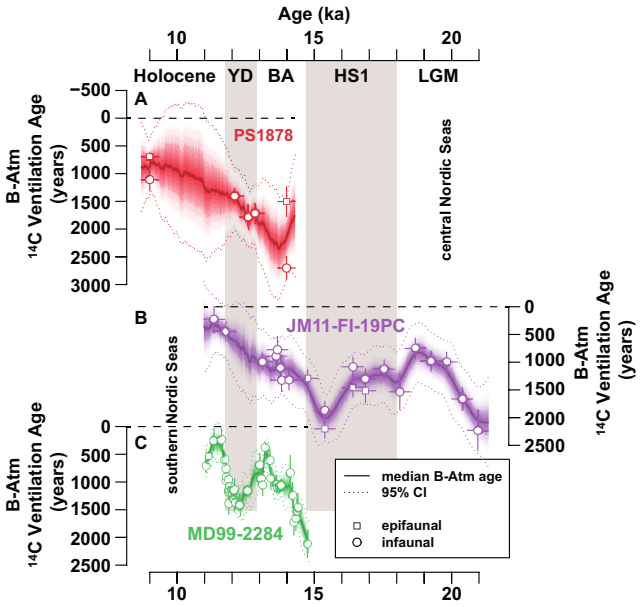

Figure 4. As in Figure 3 for Benthic-Atmosphere (B-Atm) ventilation age estimates of cores (a) PS878, (b) JM11-FI-19PC, and (c) MD99-2284. Datapoints of epifaunal and infaunal benthic foraminifera are marked with squares and circles, respectively. Stratigraphic units are indicated at the top. BA, Bølling-Allerød interstadial; HS1, Heinrich Stadial 1; LGM, Last Glacial Maximum; YD, Younger Dryas stadial.

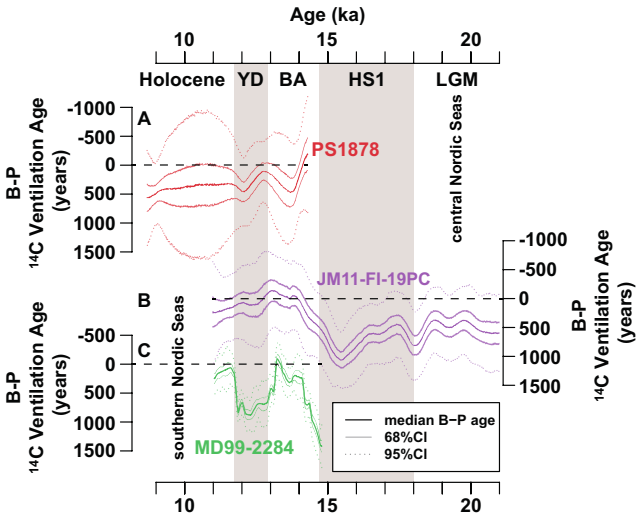

Figure 5. Benthic-Planktic (B–P) offset of cores (a) PS878, (b) JM11-FI-19PC, and (c) MD99-2284 based on ventilation estimates in Figures 3 and 4. Lines denote the posterior median value and pointwise 68% and 95% credible intervals. Stratigraphic units are indicated at the top. BA, Bølling-Allerød interstadial; HS1, Heinrich Stadial 1; LGM, Last Glacial Maximum; YD, Younger Dryas stadial.

P-Atm values of the PS1878 record remained >1,500 ^{14}C years throughout the BA (Figure 3a). The described discrepancies between the records (especially between the two southernmost records) indicate that the ventilation of subsurface waters shows substantial spatial variability, suggesting that it highly depends on local conditions such as, for example, sea ice and meltwater volume.

The B-Atm ventilation ages decreased in the southern Nordic Seas records over the BA interstadial from c. 2,000 ^{14}C years to c. 1,000 ^{14}C years. Together with the increase in P-Atm values, this resulted in the B-P offset decreasing to c. 0 ^{14}C years (Figures 5b and 5c), revealing intensive exchange between the surface and deep ocean. Despite the weak subsurface water ventilation most probably caused by abundant meltwaters from the retreating ice sheets (e.g., Rüther et al., 2012), the low B-P offset indicates a rapid reactivation of meridional circulation in the southern Nordic Seas at the onset of the BA interstadial, as suggested earlier by Ezat et al. (2017), McManus et al. (2004) and Stanford et al. (2011).

In the PS1878 record of the early BA interstadial, two different benthic foraminiferal species gave significantly diverging results. Epibenthic *C. wuellerstorfi* yielded ^{14}C age younger than the co-occurring planktic *N. pachyderma*. Negative B-P offsets have previously been observed in the western Iceland Sea between 15 and 25 ka (Voelker et al., 2000). However, the B_{Ou}-Atm value from the same sample is much higher than the B_{Cw}-Atm value. Taking into account that the ^{14}C age of *C. wuellerstorfi* might be influenced by the very low abundance of this species (Telesiński, Spielhagen, & Bauch 2014) or by modern radiocarbon contamination (Muschitiello et al., 2019), we find the ^{14}C age of *O. umbonatus* and the ventilation ages derived from it more reliable. The B_{Ou}-Atm value of c. 2,700 ^{14}C years at 14 ka is the highest in all three records and indicates extremely weak ventilation of bottom waters in the central Greenland Sea during the early BA. Even though the ventilation rapidly improved over the interstadial, it remained significantly weaker than in the southern Norwegian Sea which might be caused not only by the distal location of this site but also the significantly greater water depth. Nevertheless, at the BA/YD boundary, the B-P offset was low (Figure 5a), which might indicate the onset of deep convection in the central Greenland Sea. The gradient of the ventilation strength between the southern and the central Nordic Seas resembles the delay in AW advection into the central Nordic Seas over the early Holocene (e.g., Telesiński et al., 2015), caused by a deglacial freshwater input from the Greenland Ice Sheet (GIS) (Blaschek & Renssen, 2013). During the BA interstadial, the influence of GIS meltwaters must have been even stronger than during the Holocene, preventing the central Nordic Seas from reaching a modern-like circulation pattern and potentially pushing the convection center farther south.

During the YD stadial, the P-Atm offsets in the southern Nordic Seas were low and close to modern values. In the central part of the basin, they decreased from c. 1,700 ^{14}C years to c. 1,000 ^{14}C years over this interval (Figure 3). The B-P offsets increased, especially in cores PS1878 and MD99-2284 (Figure 5), indicating a disturbance in overturning circulation. Over this interval, the Nordic Seas were affected by freshwater intrusions originating either from the Arctic (e.g., Condron & Winsor, 2012; Telesiński et al., 2015) or from the Fennoscandian Ice Sheet (e.g., Dokken et al., 2013; Muschitiello et al., 2015, 2016). The freshwater lid in the central Nordic Seas must have been strong enough to perturb

deepwater formation at least transiently (Bauch et al., 2001; McManus et al., 2004). On the other hand, the presence of freshwater enhanced sea-ice (Cabedo-Sanz et al., 2013; Müller et al., 2009) and brine formation (Thornalley et al., 2011). The latter could explain the improved mixing of the upper water column and low P-Atm ventilation ages.

At the onset of the Holocene, the P-Atm and B-Atm ventilation ages both in the central and southern Nordic Seas decreased, reaching values close to modern. This confirms that already in the early Holocene the circulation in the Nordic Seas became similar to today (e.g., Thornalley et al., 2015; Waelbroeck et al., 2001).

4. Summary and Conclusions

The comparison of four planktic records from the Nordic Seas covering the last deglaciation reveals generally consistent variations in P-Atm reservoir ages over most of the studied period, albeit important spatial variability exists in some intervals (e.g., during the BA interstadial, Figure 3). The significant differences in the P-Atm records suggest that the ventilation of subsurface waters was strongly influenced by local conditions such as, for example, sea-ice and meltwater input, changes in mixed-layer depth, and/or changing contributions of water masses with different ^{14}C signatures. Marine radiocarbon dates, especially of planktic microfossils, are commonly used to constrain marine chronologies. They are usually corrected for the globally averaged ocean-atmosphere reservoir age offset ($R = 405$ years; Reimer et al., 2013), sometimes taking into account a regional difference (ΔR), constant in time. Our results clearly show that a strong variability in planktic reservoir ages might occur both in time and in space, even within a relatively small area such as the central and southern Nordic Seas. These fluctuations should be taken into account when constructing radiocarbon-based age models in the future.

The changes in benthic ventilation ages, though of higher amplitude than their planktic counterparts, seem to exhibit a more consistent general pattern, with high values in HS1 and the YD stadial and low values during the BA interstadial and the Holocene. The PS1878 record differs the most from the other records, for example, over the BA interstadial, where ages are much older than in the records from shallower, more southerly sites. As the presented records cover a large range of water depth, from 1,179 m (JM11-FI-19PC) to 3,048 m (PS1878), the general coherence of the benthic records, compared to the planktics, suggests that the deep Nordic Seas have been generally bathed by a single water mass analogous to the present-day Greenland Sea Deep Water (Marshall & Schott, 1999). Changes in benthic ventilation ages reflect variations in the renewal of this deepwater mass and were directly related to the intensity of deepwater formation (deep convection) in the Nordic Seas and the overflows into the North Atlantic. They were therefore directly linked to regional shifts in ocean circulation and millennial-scale climate changes. Taking into account significant offsets in ventilation ages between different benthic species (not only miliolid vs. nonmiliolid but also, e.g., epifaunal vs. infaunal nonmiliolid species), we recommend using, if possible, narrow taxonomic or ecological groups of foraminifera for the reconstruction of bottom water ventilation.

Conflict of Interest

The authors declare no conflicts of interest relevant to this study.

Data Availability Statement

All data sets are available at https://doi.pangaea.de/10.1594/PANGAEA.929246.

Acknowledgments
The study was supported by Grant No. 2016/21/D/ST10/00785 funded by the National Science Centre, Poland. M. M. Ezat was funded by the Research Council of Norway and the Co-funding of Regional, National, and International Programmes (COFUND)—Marie Skłodowska-Curie Actions under the EU Seventh Framework Programme (FP7), Project No. 274429, and the Research Council of Norway through its Centers of Excellence funding scheme, Grant No. 223259. We thank Thomas Cronin and two anonymous reviewers for their constructive criticism and suggestions which improved the manuscript.

References

Aagaard, K., Swift, J. H., & Carmack, E. C. (1985). Thermohaline circulation in the Arctic Mediterranean Seas. *J. Geophys. Res.*, *90*, 4833–4846. https://doi.org/10.1029/JC090iC03p04833

Adkins, J. F., & Boyle, E. A. (1997). Changing atmospheric Δ14C and the record of deep water paleoventilation ages. *Paleoceanography*, *12*(3), 337–344. https://doi.org/10.1029/97pa00379

Andersen, K. K., Azuma, N., Barnola, J.-M., Bigler, M., Biscaye, P., Caillon, N., et al. (2004). High-resolution record of Northern Hemisphere climate extending into the last interglacial period. *Nature*, *431*, 147–151. https://doi.org/10.1038/nature02805

Bakke, J., Lie, Ø., Heegaard, E., Dokken, T., Haug, G. H., Birks, H. H., et al. (2009). Rapid oceanic and atmospheric changes during the Younger Dryas cold period. *Nature Geoscience*, *2*, 202–205. https://doi.org/10.1038/ngeo439

Bauch, H., Erlenkeuser, H., Spielhagen, R. F., Struck, U., Matthiessen, J., Thiede, J., & Heinemeier, J. (2001). A multiproxy reconstruction of the evolution of deep and surface waters in the subarctic Nordic seas over the last 30,000yr. *Quaternary Science Reviews*, *20*, 659–678. https://doi.org/10.1016/s0277-3791(00)00098-6

Bauch, H. A., Kandiano, E. S., & Helmke, J. P. (2012). Contrasting ocean changes between the subpolar and polar North Atlantic during the past 135 ka. *Geophysical Research Letters*, *39*, L11604. https://doi.org/10.1029/2012GL051800

Blaschek, M., & Renssen, H. (2013). The Holocene thermal maximum in the Nordic Seas: The impact of Greenland Ice Sheet melt and other forcings in a coupled atmosphere-sea-ice-ocean model. *Climate of the Past*, *9*, 1629–1643. https://doi.org/10.5194/cp-9-1629-2013

Brendryen, J., Haflidason, H., Yokoyama, Y., Haaga, K. A., & Hannisdal, B. (2020). Eurasian Ice Sheet collapse was a major source of Meltwater Pulse 1A 14,600 years ago. *Nature Geoscience*, (3), 1–6. https://doi.org/10.1038/s41561-020-0567-4

Broecker, W. S. (1998). Paleocean circulation during the last deglaciation: A bipolar seesaw? *Paleoceanography*, *13*(2), 119–121. https://doi.org/10.1029/97PA03707

Cabedo-Sanz, P., Belt, S. T., Knies, J., & Husum, K. (2013). Identification of contrasting seasonal sea ice conditions during the Younger Dryas. *Quaternary Science Reviews*, *79*, 74–86. https://doi.org/10.1016/j.quascirev.2012.10.028

Clark, P. U., Shakun, J. D., Baker, P. A., Bartlein, P. J., Brewer, S., Brook, E., et al. (2012). Global climate evolution during the last deglaciation. *Proceedings of the National Academy of Sciences of the United States of America*, *109*(19). https://doi.org/10.1073/pnas.1116619109

CLIMAP Project Members. (1976). The Surface of the Ice-Age Earth. *Science*, *191*(4232), 1131–1137.

Condron, A., & Winsor, P. (2012). Meltwater routing and the Younger Dryas. *Proceedings of the National Academy of Sciences*, *109*(49), 19928–19933. https://doi.org/10.1073/pnas.1207381109

Dansgaard, W., Johnsen, S. J., Clausen, H. B., Dahl-Jensen, D., Gundestrup, N. S., Hammer, C. U., et al. (1993). Evidence for general instability of past climate from a 250-kyr ice-core record. *Nature*, *364*, 218–220. https://doi.org/10.1038/364218a0

Dickson, R., Lazier, J., Meincke, J., Rhines, P., & Swift, J. (1996). Long-term coordinated changes in the convective activity of the North Atlantic. *Progress in Oceanography*, *38*(3), 241–295. https://doi.org/10.1016/s0079-6611(97)00002-5

Dickson, R. R., & Brown, J. (1994). The production of North Atlantic deep water: Sources, rates, and pathways. *Journal of Geophysical Research*, *99*(C6), 12319–12341. Retrieved from http://onlinelibrary.wiley.com/doi/10.1029/94JC00530/full

Dokken, T. M., Nisancioglu, K. H., Li, C., Battisti, D. S., & Kissel, C. (2013). Dansgaard-Oeschger cycles: Interactions between ocean and sea ice intrinsic to the Nordic seas. *Paleoceanography*, *28*, 491–502. https://doi.org/10.1002/palo.20042

Ezat, M. M., Rasmussen, T. L., & Groeneveld, J. (2014). Persistent intermediate water warming during cold stadials in the southeastern Nordic seas during the past 65 k.y.*Geology*, *42*(8), 663–666. https://doi.org/10.1130/G35579.1

Ezat, M. M., Rasmussen, T. L., & Groeneveld, J. (2016). Reconstruction of hydrographic changes in the southern Norwegian Sea during the past 135 kyr and the impact of different foraminiferal Mg/Ca cleaning protocols. *Geochemistry, Geophysics, Geosystems*, *17*, 3420–3436. https://doi.org/10.1002/2016GC006325

Ezat, M. M., Rasmussen, T. L., Skinner, L. C., & Zamelczyk, K. (2019). Deep ocean 14C ventilation age reconstructions from the Arctic Mediterranean reassessed. *Earth and Planetary Science Letters*, *518*, 67–75. https://doi.org/10.1016/j.epsl.2019.04.027

Ezat, M. M., Rasmussen, T. L., Thornalley, D. J. R., Olsen, J., Skinner, L. C., Hönisch, B., & Groeneveld, J. (2017). Ventilation history of Nordic Seas overflows during the last (de)glacial period revealed by species-specific benthic foraminiferal14C dates. *Paleoceanography*, *32*(2), 172–181. https://doi.org/10.1002/2016PA003053

Greco, M., Jonkers, L., Kretschmer, K., Bijma, J., & Kucera, M. (2019). Variable habitat depth of the planktonic foraminifera *Neogloboquadrina pachyderma* in the northern high latitudes explained by sea-ice and chlorophyll concentration. *Biogeosciences Discussions*, 1–30. https://doi.org/10.5194/bg-2019-79

Hansen, B., & Østerhus, S. (2000). North Atlantic-Nordic seas exchanges. *Progress in Oceanography*, *45*, 109–208. https://doi.org/10.1016/S0079-6611(99)00052-X

Håvik, L., Pickart, R. S., Torres, D., Thurnherr, A. M., Beszczynska-Möller, A., Walczowski, W., & von Appen, W.-J. (2017). Evolution of the East Greenland current from Fram Strait to Denmark Strait: Synoptic measurements from summer 2012. *Journal of Geophysical Research: Oceans*, *122*. https://doi.org/10.1002/2016JC012336

Heier-Nielsen, S., Conradsen, K., Heinemeier, J., Knudsen, K. L., Nielsen, H. L., Rud, N., & Sveinbjörnsdóttir, Á. E. (1995). Radiocarbon dating of shells and foraminifera from the Skagen Core, Denmark: evidence of reworking. *Radiocarbon*, *37*(2), 119–130. https://doi.org/10.1017/s0033822200030551

Hoff, U., Rasmussen, T. L., Stein, R., Ezat, M. M., & Fahl, K. (2016). Sea ice and millennial-scale climate variability in the Nordic seas 90 kyr ago to present. *Nature Communications*, *7*, 12247. https://doi.org/10.1038/ncomms12247

Mangerud, J., Bondevik, S., Gulliksen, S., Karin Hufthammer, A., & Høisæter, T. (2006). Marine 14C reservoir ages for 19th century whales and molluscs from the North Atlantic. *Quaternary Science Reviews*, *25*(23–24), 3228–3245. https://doi.org/10.1016/j.quascirev.2006.03.010

Marshall, J., & Schott, F. (1999). Open-ocean convection: Observations, theory, and models. *Reviews of Geophysics*, *37*(1), 1–64. https://doi.org/10.1029/98rg02739 Retrieved from http://www.math.nyu.edu/caos_teaching/ocean_dynamics/reading/marshall_schott99.pdf

McManus, J. F., Francois, R., Gherardi, J.-M., Keigwin, L. D., & Brown-Leger, S. (2004). Collapse and rapid resumption of Atlantic meridional circulation linked to deglacial climate changes. *Nature*, *428*, 834–837. https://doi.org/10.1038/nature02494

Müller, J., Massé, G., Stein, R., & Belt, S. T. (2009). Variability of sea-ice conditions in the Fram Strait over the past 30,000 years. *Nature Geoscience*, *2*(11), 772–776. https://doi.org/10.1038/ngeo665

Muschitiello, F., D'Andrea, J., Schmittner, A., Heaton, T. J., Balascio, N. L., et al. (2019). Deep-water circulation changes lead North Atlantic climate during deglaciation. *Nature Communications*, *10*, 1272. https://doi.org/10.1038/s41467-019-09237-3

Muschitiello, F., Lea, J. M., Greenwood, S. L., Nick, F. M., Brunnberg, L., Macleod, A., & Wohlfarth, B. (2016). Timing of the first drainage of the Baltic Ice Lake synchronous with the onset of Greenland Stadial 1. *Boreas*, *45*(2), 322–334. https://doi.org/10.1111/bor.12155

Muschitiello, F., O'Regan, M., Martens, J., West, G., Gustafsson, Ö., & Jakobsson, M. (2020). A new 30 000-year chronology for rapidly deposited sediments on the Lomonosov Ridge using bulk radiocarbon dating and probabilistic stratigraphic alignment. *Geochronology*, *2*(1), 81–91. https://doi.org/10.5194/gchron-2-81-2020

Muschitiello, F., Pausata, F. S. R., Watson, J. E., Smittenberg, R. H., Salih, A. A. M., Brooks, S. J., et al. (2015). Fennoscandian freshwater control on Greenland hydroclimate shifts at the onset of the Younger Dryas. *Nature Communications*, *6*, 8939. https://doi.org/10.1038/ncomms9939

Olsen, J., Rasmussen, T. L., & Reimer, P. J. (2014). North Atlantic marine radiocarbon reservoir ages through Heinrich event H4: A new method for marine age model construction. *Geological Society, London, Special Publications*, *398*(1), 95–112. https://doi.org/10.1144/SP398.2

Rasmussen, T. L., Thomsen, E., Labeyrie, L., & van Weering, T. C. E. (1996). Circulation changes in the Faeroe-Shetland Channel correlating with cold events during the last glacial period (58-10 ka). *Geol*, *24*, 937–940. https://doi.org/10.1130/0091-7613(1996)024<0937:CCITFS>2.3.CO;2

Reimer, P. J., Bard, E., Bayliss, A., Beck, J. W., Blackwell, P. G., Ramsey, C. B., et al. (2013). IntCal13 and Marine13 radiocarbon age calibration curves 0-50,000 Years cal BP. *Radiocarbon*, *55*(4), 1869–1887. https://doi.org/10.2458/azu_js_rc.55.16947

Rudels, B., & Quadfasel, D. (1991). Convection and deep water formation in the Arctic Ocean-Greenland Sea System. *Journal of Marine Systems*, *2*(3–4), 435–450. https://doi.org/10.1016/0924-7963(91)90045-V

Rüther, D. C., Bjarnadóttir, L. R., Junttila, J., Husum, K., Rasmussen, T. L., Lucchi, R. G., & Andreassen, K. (2012). Pattern and timing of the northwestern Barents Sea Ice Sheet deglaciation and indications of episodic Holocene deposition. *Boreas*, *41*(3), 494–512. https://doi.org/10.1111/j.1502-3885.2011.00244.x

Sarnthein, M., Jansen, E., Weinelt, M., Arnold, M., Duplessy, J. C., Erlenkeuser, H., et al. (1995). Variations in Atlantic surface ocean paleoceanography, 50°-80°N: A time-slice record of the last 30,000 years. *Paleoceanography*, *10*(6), 1063–1094. https://doi.org/10.1029/95pa01453

Shakun, J. D., Clark, P. U., He, F., Marcott, S. A., Mix, A. C., Liu, Z., et al. (2012). Global warming preceded by increasing carbon dioxide concentrations during the last deglaciation. *Nature*, *484*, 49–54. https://doi.org/10.1038/nature10915

Skinner, L. C., Muschitiello, F., & Scrivner, A. E. (2019). Marine reservoir age variability over the last deglaciation : Implications for marine carbon cycling and prospects for regional radiocarbon calibrations. *Paleoceanography and Paleoclimatology*, *34*. https://doi.org/10.1029/2019PA003667

Skinner, L. C., & Shackleton, N. J. (2004). Rapid transient changes in northeast Atlantic deep water ventilation age across Termination I. *Paleoceanography*, *19*, 11. https://doi.org/10.1029/2003PA000983

Skinner, L. C., Waelbroeck, C., Scrivner, A. E., & Fallon, S. J. (2014). Radiocarbon evidence for alternating northern and southern sources of ventilation of the deep Atlantic carbon pool during the last deglaciation. *Proceedings of the National Academy of Sciences*, *111*(15), 5480–5484. https://doi.org/10.1073/pnas.1400668111

Stanford, J. D., Rohling, E. J., Bacon, S., Roberts, A. P., Grousset, F. E., & Bolshaw, M. (2011). A new concept for the paleoceanographic evolution of Heinrich event 1 in the North Atlantic. *Quaternary Science Reviews*, *30*(9–10), 1047–1066. https://doi.org/10.1016/j.quascirev.2011.02.003

Stern, J. V., & Lisiecki, L. E. (2013). North Atlantic circulation and reservoir age changes over the past 41,000 years. *Geophysical Research Letters*, *40*, 3693–3697. https://doi.org/10.1002/grl.50679

Swift, J. H. (1986). The Arctic waters. In B. Hurdle (Ed.), *The Nordic Seas* (pp. 129–151). Springer.

Telesiński, M. M., Bauch, H. A., Spielhagen, R. F., & Kandiano, E. S. (2015). Evolution of the central Nordic Seas over the last 20 thousand years. *Quaternary Science Reviews*, *121*, 98–109. https://doi.org/10.1016/j.quascirev.2015.05.013

Telesiński, M. M., Spielhagen, R. F., & Bauch, H. A. (2014). Water mass evolution of the Greenland Sea since late glacial times. *Climate of the Past*, *10*, 123–136. https://doi.org/10.5194/cp-10-123-2014

Telesiński, M. M., Spielhagen, R. F., & Lind, E. M. (2014). A high-resolution Lateglacial and Holocene paleoceanographic record from the Greenland Sea. *Boreas*, *43*(2), 273–285. https://doi.org/10.1111/bor.12045

Thibodeau, B., Bauch, H. A., & Pedersen, T. F. (2017). Stratification-induced variations in nutrient utilization in the Polar North Atlantic during past interglacials. *Earth and Planetary Science Letters*, *457*, 127–135. https://doi.org/10.1016/j.epsl.2016.09.060

Thornalley, D. J. R., Barker, S., Broecker, W. S., Elderfield, H., & McCave, I. N. (2011). The deglacial evolution of North Atlantic deep convection. *Science*, *331*, 202–205. https://doi.org/10.1126/science.1196812

Thornalley, D. J. R., Bauch, H. A., Gebbie, G., Guo, W., Ziegler, M., Bernasconi, S. M., et al. (2015). A warm and poorly ventilated deep Arctic Mediterranean during the last glacial period. *Science*, *349*(6249), 706–710. https://doi.org/10.1126/science.aaa9554 Retrieved from http://science.sciencemag.org/content/349/6249/706.full

Voelker, A. H. L., Grootes, P. M., Nadeau, M.-J., & Sarnthein, M. (2000). Radiocarbon levels in the Iceland Sea from 25-53 kyr and their link to the Earth's magnetic field intensity. *Radiocarbon*, *42*(3), 437–452. https://doi.org/10.1017/s0033822200030368

Vorren, T. O., & Plassen, L. (2002). Deglaciation and palaeoclimate of the Andfjord-Vagsfjord area, North Norway. *Sbor*, *31*(2), 97–125. https://doi.org/10.1080/030094802320129926

Waelbroeck, C., Duplessy, J.-C., Michel, E., Labeyrie, L., Paillard, D., & Duprat, J. (2001). The timing of the last deglaciation in North Atlantic climate records. *Nature*, *412*, 724–727. https://doi.org/10.1038/35089060